Journal of Metals, Materials and Minerals, 37(1), e2738, 2027

Electrospun polyvinyl alcohol nanofibrous membranes incorporated with silver nanowires and sambiloto (*andrographis paniculata nees*) for wound healing applications

Junaidi JUNAIDI[1,*], Chandra PRATIWI[1], Yanti YULIANTI[1], Roniyus MARJUNUS[1], Sutopo HADI[2], and Khairurrijal KHAIRURRIJAL[3,4]

[1] *Department of Physics, Faculty of Mathematics and Natural Sciences, University of Lampung, Jl. Sumantri Brojonegoro No. 1 Gedong Meneng Rajabasa Bandar Lampung, Lampung, 35145, Indonesia*

[2] *Department of Chemistry, Faculty of Mathematics and Natural Sciences, University of Lampung, Jl. Sumantri Brojonegoro No. 1 Gedong Meneng Rajabasa Bandar Lampung, Lampung, 35145, Indonesia*

[3] *Department of Physics, Faculty of Mathematics and Natural Sciences, Institut Teknologi Bandung, Jalan Ganesa 10, Bandung, West Java, 40132, Indonesia*

[4] *Research Center for Biosciences and Biotechnology, Institute for Research and Community Services, Jalan Ganesa 10, Bandung, West Java, 40132, Indonesia*

***Corresponding author e-mail**: junaidi.1982@fmipa.unila.ac.id

Received date:
10 May 2026
Revised date:
21 July 2026
Accepted date:
23 October 2026

Keywords:
Silver nanowires;
Sambiloto;
Polyvinyl alcohol;
Polyvinyl pyrrolidone;
Electrospinning

Abstract

A new variation of wound covering nanofibrous membranes synthesized using electrospinning method from mixtures of polyvinyl alcohol (PVA), silver nanowires (AgNWs), and sambiloto (*Andrographis paniculata* Nees) leaves has successfully been developed for antibacterial applications. Four variations of nanofibrous membranes, namely pure PVA, PVA and sambiloto (PVA/S), PVA and silver nanowires (PVA/AgNWs), as well as PVA, sambiloto, and silver nanowires (PVA/S/AgNWs) were prepared and preclinically tested on white mice (*Mus muscullus*) that had previously been injured. The FTIR spectrum wavenumbers of PVA/S, PVA/AgNWs, and PVA/S/AgNWs for the (O–H) functional group experienced a shift greater (shifted left) than PVA. For the SEM images, the minimum diameter of the membrane nanofiber was 122 nm, while the maximum was 257 nm. The results showed that wound healing in the mice occurred after 72 h, while the PVA/S/AgNWs membranes demonstrated a more complete and accelerated wound closure than other membranes. Furthermore, the potential of sambiloto as an ingredient in a wound covering drug is relatively large. Sambiloto is an andrographolide compound used to fight disease due to its antibacterial power as well as the potential to activate lymphocytes and produce antibodies and silver has been used extensively in clinical equipment as an antimicrobial.

1. Introduction

An injury or wound is defined as a disruption or loss of skin and epithelial integrity that can result from various causes, including surgical procedures, trauma, burns, and accidental incisions. Although many acute wounds can heal naturally through a series of coordinated biological processes, including hemostasis, inflammation, proliferation, and tissue remodeling, inadequate wound management may increase the risk of microbial infection and delay tissue regeneration. Wound infection is one of the major complications that can interfere with normal healing and may lead to prolonged inflammation, tissue damage, and, in severe cases, systemic complications [1–2]. Therefore, the development of effective wound dressing materials that can protect the wound, maintain an appropriate microenvironment, and support tissue regeneration remains an important area of biomedical research [3,4].

Conventional wound dressings, such as cotton gauze, are widely used to protect wounds from external contamination and absorb wound exudate. However, conventional gauze has several limitations, including poor moisture regulation and the tendency to adhere to newly formed tissue, which may cause pain and secondary tissue damage during dressing changes and potentially delay the healing process. Traditional dry or wet gauze dressings primarily provide physical protection and do not necessarily address the complex biological processes involved in wound repair. In contrast, modern wound dressing strategies aim to maintain a moist wound environment, which can facilitate epithelial cell proliferation and migration, promote autolytic debridement, and support tissue regeneration [5]. The concept of moist wound healing was established by Winter, who demonstrated that a moist environment can promote faster epithelialization compared with wounds allowed to dry and form a scab. These developments have encouraged the design of advanced wound dressings that not only function as physical barriers but also provide active biological functions, including anti-microbial, antioxidant, anti-inflammatory, and tissue-regenerative activities [3,4,6].

Natural plant extracts have attracted considerable attention as functional components of advanced wound dressing systems because they contain diverse bioactive phytochemicals, including flavonoids, phenolic compounds, terpenoids, alkaloids, and other secondary

metabolites. These compounds may exhibit multiple biological activities relevant to different stages of wound healing, including antioxidant, antimicrobial, anti-inflammatory, and immunomodulatory effects. The wound healing process is regulated by a complex interaction among inflammatory cells, cytokines, growth factors, extracellular matrix components, and tissue-specific cells. Growth factors and cytokines play important roles in regulating inflammation, cell proliferation, migration, angiogenesis, and extracellular matrix remodeling during tissue repair [7]. Therefore, plant-derived bioactive compounds with antioxidant and anti-inflammatory properties may help regulate the wound microenvironment and support the progression of tissue repair. The incorporation of plant extracts into polymeric and nanofibrous wound dressings is consequently considered a promising strategy for developing multifunctional biomaterials that combine structural support with therapeutic biological activity [8].

Among medicinal plants, sambiloto (Andrographis paniculata Nees) has attracted considerable interest because of its rich phytochemical composition and broad pharmacological activities. Sambiloto contains several bioactive diterpenoid lactones, particularly andrographolide, together with flavonoids and other phytochemical constituents [9]. Andrographolide is considered one of the major bioactive compounds responsible for the pharmacological properties of sambiloto The plant and its constituents have been investigated for various biological activities, including anti-inflammatory, antioxidant, antimicrobial, immunomodulatory, and hepatoprotective effects [9,10]. The anti-inflammatory activity of sambiloto is particularly relevant to wound healing because excessive or prolonged inflammation can interfere with the progression of tissue repair and the transition toward the proliferative and remodeling phases [1,7]. In addition, its antioxidant activity may help regulate oxidative stress by reducing excessive reactive oxygen species (ROS), while its antimicrobial properties may contribute to controlling microbial contamination at the wound site [10]. Therefore, the multifunctional biological properties of sambiloto make it a promising candidate as a plant-derived functional component in advanced wound dressing materials.

The incorporation of sambiloto extract into a nanofibrous membrane may provide additional biological functions beyond those offered by a conventional passive wound dressing. In particular, the bioactive phytochemicals present in the extract may complement the antimicrobial properties of silver-based nanomaterials. Silver nanowires (AgNWs) have attracted significant attention because of their unique electrical, optical, and antimicrobial properties, with applications in flexible electronics, sensors, optoelectronic devices, and biomedical materials. The unique properties of AgNWs are strongly associated with their one-dimensional morphology, high aspect ratio, excellent electrical conductivity, and optical characteristics, which have led to their extensive investigation for flexible and transparent conductive applications [11–13]. The antimicrobial activity of silver-based nanomaterials is generally associated with the release of Ag^+ ions and their interactions with microbial cell membranes and intracellular components, which can disrupt cellular functions and inhibit microbial growth [14,15]. Accordingly, the combination of AgNWs and sambiloto extract may provide complementary biological functions, in which AgNWs contribute primarily to antimicrobial activity while the phytochemicals from sambiloto may provide antioxidant and anti-inflammatory effects. However, a definitive synergistic interaction between these components requires direct experimental comparison and should not be assumed solely from their individual biological properties.

Electrospinning is a versatile and effective technique for fabricating polymeric, inorganic, and composite nanofibers. The technique utilizes electrostatic forces generated by applying a high voltage between a polymer solution contained in a syringe or spinneret and a grounded collector, producing continuous fibers with diameters ranging from the micro- to nanoscale [16,17]. Electrospinning has emerged as an effective approach for producing nanofibrous materials with controllable fiber morphology and high surface area. Electrospun nanofibrous membranes possess a high surface-area-to-volume ratio, interconnected porous structures, and extracellular matrix-like morphology, making them attractive for biomedical and wound dressing applications [18]. These structural characteristics can facilitate cell attachment and migration, gas exchange, nutrient transport, and moisture management, while also providing a suitable platform for incorporating bioactive compounds and nanomaterials. In addition, polymeric nanofibers fabricated by electrospinning can be designed to provide structural support while serving as carriers for active therapeutic agents. Polyvinyl alcohol (PVA), in particular, has attracted considerable attention in biomedical applications because of its hydrophilicity, film-forming ability, biocompatibility, and suitability for electrospinning. The integration of AgNWs and sambiloto extract into a PVA-based electrospun nanofibrous matrix may therefore provide a multifunctional wound dressing platform that combines the structural advantages of nanofibers with the antimicrobial potential of AgNWs and the antioxidant and anti-inflammatory properties of plant-derived bioactive compounds [19].

Based on this background, the present study aims to develop and evaluate a multifunctional electrospun nanofibrous membrane incorporating AgNWs and sambiloto leaf extract using PVA as the polymer matrix. Four membrane formulations were prepared, namely pure PVA, PVA/sambiloto extract (PVA/S), PVA/AgNWs, and PVA/sambiloto extract by AgNWs (PVA/S/AgNWs), to investigate the contribution of each component to the physicochemical and biological performance of the developed membranes. The resulting nanofibrous membranes were characterized using scanning electron microscopy (SEM) and Fourier-transform infrared spectroscopy (FTIR). Their preliminary wound healing performance was subsequently evaluated using a murine incision wound model, with observations performed at 24 h, 48 h, and 72 h to assess macroscopic wound responses, including erythema, edema, and changes in incision length. The developed membrane is expected to provide a multifunctional wound dressing platform in which the nanofibrous PVA matrix provides structural and moisture-management functions, AgNWs contribute potential antimicrobial activity, and sambiloto extract provides plant-derived bioactive compounds with potential antioxidant and anti-inflammatory functions. This integrated approach is expected to contribute to the development of advanced wound dressing materials based on the complementary properties of nanomaterials and medicinal plant extracts.

2. Materials and methods

2.1 Materials

The materials used in this study include silver nitrate ($AgNO_3$) 99% (Sigma-Aldrich Pte. Ltd., Science Park Drive, Singapore), PVP

Mw. 30,000 g·mol^{-1}, PVA Mw. 30,000 g·mol^{-1}, ethylene glycol (EG) 99.5% (Merck kGaA, Darmstadt, Germany), ethanol 96% (Merck kGaA, Darmstadt, Germany), $FeCl_3 \cdot 6H_2O$, silicon oil, deionized water, sambiloto leaves, and plaster without medicinal properties with a size of 1.25 cm × 45 cm.

2.2 Methods

2.2.1 Synthesis of AgNWs

In general, the synthesis of AgNWs using the oil bath method comprises three processes, namely the dissolving process, synthesis process, and centrifugation for separation of AgNWs [20–22]. The dissolving process began with cleaning and sterilizing the tools as well as the materials, then PVP was dissolved as a polymer capping agent, $FeCl_3 \cdot 6H_2O$ and $AgNO_3$ were dissolved in EG as solvent. Figure 1 shows the synthesis of AgNWs by polyol method.

In the polyol process, ethylene glycol serves primarily as the polyol solvent and also acts as a reducing agent for the reduction of Ag^+ to metallic Ag^0 under elevated temperature. Polyvinylpyrrolidone (PVP) acts as a capping and structure-directing agent, preferentially adsorbing onto specific crystal facets and promoting anisotropic growth of silver nanowires. $AgNO_3$ provides the Ag^+ precursor. $FeCl_3$ is added in a controlled amount to regulate the nucleation and growth process. The Fe^{3+}/Fe^{2+} redox couple can influence the reduction kinetics of Ag^+ and suppress uncontrolled nucleation, thereby promoting the formation and growth of one-dimensional silver nanostructures. Furthermore, 2.994 g of PVP were dissolved in 60 mL of EG, placed into the erlenmeyer flask, and then stirred at 350 rpm at 130°C for 1 h. $FeCl_3 \cdot 6H_2O$ (100 µL, 0.04 M) was also added to the PVP/EG mixture in the Erlenmeyer flask using a micropipette, while 24 mL of $AgNO_3$/EG solution (0.3 M) was added by dropping the solution using a syringe for 2 h (0.2 cm^3·min^{-1}). The solution was allowed to react for 2 h, while the centrifugation process was carried out 2 time at a speed of 3000 rpm for 10 min. The AgNWs precipitate produced was stored in ethanol to prevent damage.

2.2.2 Sambiloto leaves extract

For the extraction of sambiloto leaves, amount of 75 g of wet sambiloto leaves were mixed with 75 mL of distilled water with 50% concentration and then mashed using a blender. After the sample was completely smooth, it was filtered using filter paper and prepared for use. The extracting process of sambiloto leaves is shown in Figure 2.

After the AgNWs solution and sambiloto leaf extraction were carried out, the next step was to make a PVA solution with a concentration of 12 wt%. PVA solution was prepared by dissolving 4 g of PVA in 30 mL of deionized water. The mixture was heated at 90°C under continuous magnetic stirring at 350 rpm for approximately 1 h until a clear and homogeneous solution was obtained. After complete dissolution, the solution was allowed to cool naturally to room temperature while maintaining gentle stirring. The resulting PVA solution was then degassed to remove entrapped air bubbles before being used for subsequent electrospinning experiments. The PVA/S solution was prepared by mixing 1 mL of sambiloto leaves extract with 5 mL of PVA, while PVA/AgNWs was prepared by mixing 1 mL of AgNWs solution (0.3 M) into 5 mL of PVA. To prepare PVA/S/AgNWs, 1 mL of AgNWs solution (0.3 M) and 1 mL of sambiloto leaves extract with 5 mL of PVA. All processes were carried out using a stirrer at 350 rpm and a temperature of 90°C.

2.2.3 Preparation of PVA, PVA/S, PVA/AgNWs, and PVA/S/AgNWs nanofibers using electrospinning

The electrospinning process was performed using a single-nozzle electrospinning system equipped with a syringe pump, a high-voltage power supply, and a grounded flat aluminum collector. Prior to electrospinning, the prepared PVA, PVA/S, PVA/AgNWs, and PVA/AgNWs/S solutions were stirred until homogeneous and transferred into a 10 mL plastic syringe fitted with a stainless-steel needle as shown in Figure 3.

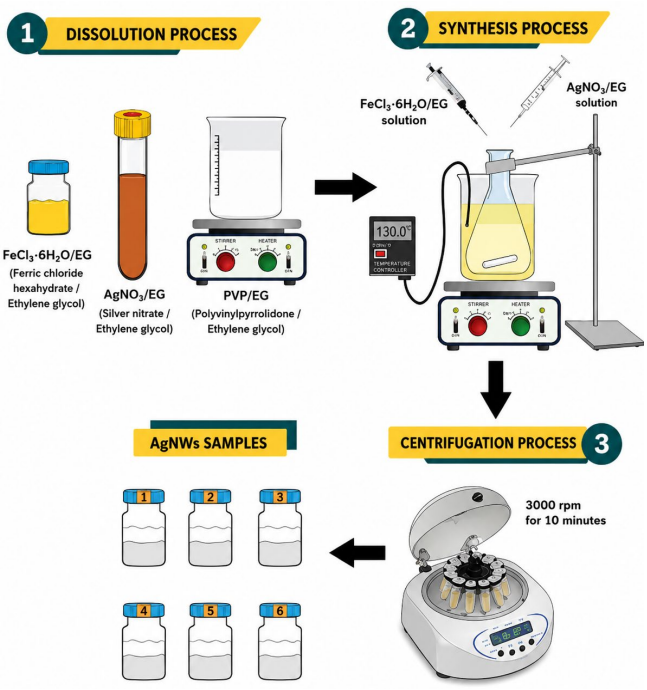


Figure 1. Synthesis of silver nanowires by polyol method.

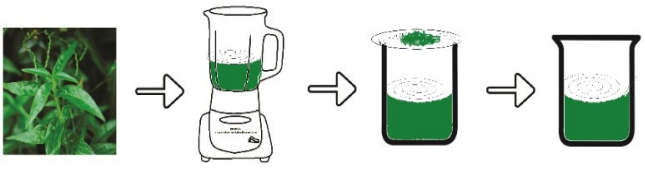


Figure 2. The extracting process of sambiloto leaves.

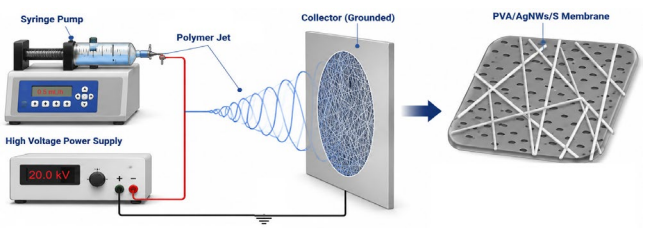


Figure 3. Electrospinning process of nanofibrous membranes.

During electrospinning, the solution was delivered at a constant flow rate of 0.5 mL·h^{-1} using a syringe pump. A positive voltage of 20 kV was applied between the needle tip and the collector, while the tip-to-collector distance was maintained at 15 cm for 6 h. Electrospinning was conducted at room temperature (25 ± 2°C) with a relative humidity of 45% to 55%. Under the applied electric field, a stable Taylor cone was formed at the needle tip, producing a continuous charged jet that elongated and underwent solvent evaporation before depositing onto the grounded collector as a nonwoven nanofibrous membrane. The same electrospinning parameters were applied for all formulations, namely PVA, PVA/S, PVA/AgNWs, and PVA/S/AgNWs, to ensure a consistent comparison of their morphological and physico-chemical properties. The electrospun nanofibrous membrane was further characterized and preclinical tests were carried in the mice.

2.2.4 Characterization

The characterization using FTIR was carried out to determine the functional groups in the four samples to be made into membranes (Shimadzu, Japan) at wavenumbers of 1000 cm^{-1} to 4000 cm^{-1}. The morphologies and size of the electrospun nanofibers are characterized using scanning electron microscopy (SEM, JSM-6390LT, JEOL) process by an acceleration voltage of 20 kV.

2.2.5 Preclinical test

The preclinical test started with the preparation of 25 male mice aged 2 to 3 month. The mice were randomly divided into 5 groups with 5 replications and placed in individual cages with food and drink at libitum (sufficiently). Moreover, they were acclimatized for 5 day, then on the day before being sliced, the hair on the back was shaved using a veet. Afterwards, antiseptic was used by administering 70% alcohol, then making an incision 1 cm to 1.2 cm long with a depth of 0.2 cm or up to the subcutis layer on the back of the mouse is done using a sterile scalpel. After each membrane was produced from the electrospinning process, the wound cover was made by attaching a 1.25 cm^2 membrane to the plaster. Finally, the plaster was used to cover wounds on the mice that had been previously injured.

3. Results and discussion

3.1 FTIR analysis

FTIR characterization is used to identify functional groups in a compound, each absorption at a particular wavelength describes the presence of a specific functional group. When a material is irradiated with infrared radiation, an interaction occurs in the form of energy absorption by atoms or molecules of the material. The absorption of infrared radiation energy causes an increase in the amplitude of the vibrations of the atoms in a molecule. The FTIR spectra for functional groups and wave numbers are shown in Figure 4 and Table 1.

Fourier-transform infrared (FTIR) spectroscopy was employed to investigate the functional groups and possible molecular interactions in the electrospun nanofibrous membranes, namely PVA, PVA/S, PVA/AgNWs, and PVA/S/AgNWs. As shown in Figure 4, all four samples exhibit a broad absorption band in the region of approximately 3250 cm^{-1} to 3265 cm^{-1}, which is attributed primarily to the stretching vibration of hydroxyl (O–H) groups. The presence of this characteristic band is consistent with the chemical structure of PVA, which contains abundant hydroxyl groups along its polymer backbone. Similar FTIR characteristics have been reported for PVA–based wound dressing materials, in which the broad band around 3260 cm^{-1} to 3300 cm^{-1} is assigned to O–H stretching vibrations associated with intermolecular and intramolecular hydrogen bonding [23,24].

For the pure PVA nanofiber Figure 4(a) the O–H stretching band is centered at approximately 3250 cm^{-1}. This broad band indicates the presence of hydroxyl groups and hydrogen-bonding interactions between PVA chains. The abundance of hydroxyl groups contributes to the hydrophilic nature of PVA, which is an advantageous property for wound dressing applications because it can facilitate interaction with wound exudate and help maintain a moist microenvironment. A controlled moist environment is generally considered beneficial for cell migration and re-epithelialization during wound healing. However, the highly hydrophilic nature of PVA may also result in excessive swelling or rapid dissolution in an aqueous environment; therefore, the physical and chemical stability of PVA-based wound dressings needs to be considered when designing materials for biomedical applications [24,25].

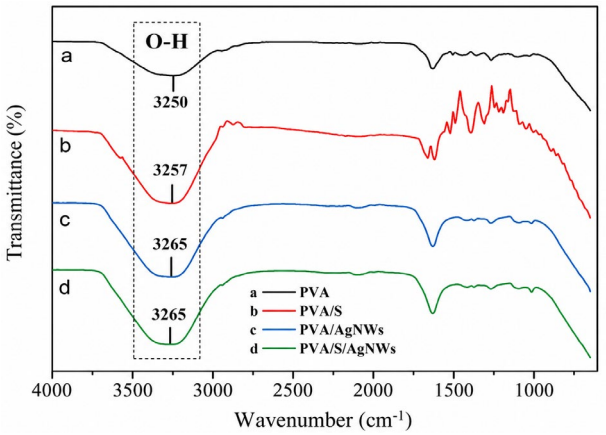


Figure 4. FTIR spectra of PVA, PVA/S, PVA/AgNWs, and PVA/S/AgNWs.

Table 1. The wave number and functional groups in each nanofiber sample.

Functional groups	Wave number [cm^{-1}]			
	PVA	PVA/S	PVA/AgNWs	PVA/S/AgNWs
O–H	3250	3257	3265	3265
C≡C	2102	2124	2117	2117
C=C	1640	1669	1640	1640
C–H	1461	1401	1416	1416
C–O	1267	1312	1274	1274

The FTIR spectrum of PVA/S in Figure 4(b) shows a broad O–H absorption band centered at approximately 3257 cm^{-1}, accompanied by a change in the shape and position of the band relative to pure PVA. The shift from 3250 cm^{-1} to 3257 cm^{-1} suggests that incorporation of sambiloto extract modifies the hydrogen-bonding environment within the PVA matrix. The plant extract contains various bioactive phytochemicals, and functional groups associated with hydroxyl, carbonyl, carboxylic acid, alkane, and ether groups have been reported in sambiloto extracts and compounds related to andrographolide. Thus, the change in the O–H band may be attributed to hydrogen bonding between hydroxyl groups of PVA and oxygen-containing functional groups from phytochemical constituents in the sambiloto extract. Such interactions may contribute to the physical incorporation and distribution of the plant-derived compounds within the polymeric nanofiber matrix [26,27].

The incorporation of sambiloto extract is particularly relevant to the development of multifunctional wound dressing materials. Sambiloto contains bioactive constituents, including diterpenoid lactones such as andrographolide and other phytochemicals, which have been associated with various biological activities [28]. The presence of oxygen-containing functional groups in these compounds may facilitate molecular interactions with the hydroxyl-rich PVA matrix. Therefore, the FTIR result provides evidence that the sambiloto extract is incorporated into the PVA nanofibrous structure, although FTIR alone cannot definitively establish the specific molecular identity or quantify the amount of individual phytochemicals present [26].

For the PVA/AgNWs nanofiber in Figure 4(b), the O–H stretching band appears at approximately 3265 cm^{-1}. The shift of the O–H band from 3250 cm^{-1} in PVA to 3265 cm^{-1} following the incorporation of AgNWs indicates a modification of the local chemical environment of the hydroxyl groups. This observation may be associated with interactions at the PVA–AgNW interface, including changes in the hydrogen-bonding network and possible interactions between oxygen-containing groups in PVA and the silver surface. Similar studies of PVA–silver composites have reported changes in the O–H region following silver incorporation, although other investigations have also observed minimal peak displacement, indicating that silver may be physically embedded within the polymer matrix rather than forming strong covalent chemical bonds. Therefore, the observed shift in the present study should be interpreted as evidence of changes in the local molecular environment rather than definitive proof of a specific Ag–O covalent bond [24].

The PVA/S/AgNWs nanofiber in Figure 4(d) also exhibits an O–H band at approximately 3265 cm^{-1}, similar to the PVA/AgNWs sample. This result indicates that the simultaneous incorporation of sambiloto extract and AgNWs is associated with a modified hydroxyl environment within the PVA matrix. The similarity of the O–H position between PVA/AgNWs and PVA/S/AgNWs suggests that the incorporation of AgNWs contributes substantially to the observed O–H vibrational environment, while the sambiloto extract may provide additional oxygen-containing functional groups and hydrogen-bonding interactions [23,26,28]. However, the absence of a new, clearly separated O–H peak does not by itself demonstrate that all components are uniformly distributed at the molecular level. Additional characterization techniques, such as X-ray photoelectron spectroscopy (XPS), would be required to provide more direct evidence of interfacial chemical interactions.

Importantly, the FTIR spectra do not show the emergence of a strong new absorption band that would indicate the formation of an entirely new chemical structure following the incorporation of AgNWs and sambiloto extract. This observation suggests that the fabrication process primarily results in physical incorporation and intermolecular interactions among PVA, the plant-derived compounds, and AgNWs, rather than extensive covalent chemical modification of the PVA backbone. Similar behavior has been reported for silver-containing PVA-based nanofibers, where the incorporation of silver did not necessarily produce major changes in the characteristic FTIR bands of the polymer, suggesting that silver species can be physically entrapped within the polymeric scaffold or interact through weak interfacial forces [23,24].

From the perspective of wound dressing applications, the FTIR results demonstrate that the PVA/S/AgNWs membrane integrates three functional components within a single nanofibrous platform. PVA provides the hydrophilic polymeric matrix and structural framework, while the sambiloto extract introduces plant-derived bioactive compounds that may contribute antioxidant and anti-inflammatory functions [26–28]. Meanwhile, AgNWs provide a silver-based functional component with potential antimicrobial activity. Silver-based materials are widely investigated for antimicrobial wound dressings because their antimicrobial effects can involve silver-ion release and interactions with microbial cell membranes and intracellular components. Silver-containing PVA-based fibrous wound dressings have also been investigated in preclinical studies combining structural properties with antibacterial and wound-healing functions [29-30].

Therefore, the combination of bitter leaf extract and AgNWs may be very promising for the treatment of infected wounds. AgNWs are expected to contribute to antimicrobial protection, while the bioactive compounds from bitter leaf may provide complementary biological effects. However, it should be emphasized that FTIR results alone cannot prove antibacterial activity or demonstrate a synergistic interaction between AgNWs and bitter leaf extract. Direct antibacterial assays, such as zone of inhibition measurements, bacterial colony-forming unit (CFU) counts, minimum inhibitory concentrations (MICs), or bacterial viability assays, are necessary to establish antimicrobial efficacy. Similarly, the synergistic effect must be experimentally demonstrated by comparing the combined system with individual PVA/S and PVA/AgNWs formulations under identical experimental conditions. Such assays have not been conducted at the current stage. This study focuses more on the initial preclinical testing of the wound dressing applied for wound healing in white mice [28].

Overall, the FTIR results indicate that the incorporation of sambiloto extract and AgNWs modifies the molecular environment of the PVA nanofibrous matrix, as evidenced particularly by the shift of the O–H stretching band from 3250 cm^{-1} for PVA to 3257 cm^{-1} for PVA/S and 3265 cm^{-1} for both PVA/AgNWs and PVA/S/AgNWs. These spectral changes support the successful integration of the functional components into the PVA nanofibers and suggest the presence of intermolecular interactions within the composite system [29]. The resulting PVA/S/AgNWs nanofibrous membrane therefore

represents a promising multifunctional platform for wound dressing applications, combining the hydrophilic and fibrous characteristics of PVA with the potential bioactivity of sambiloto extract and the antimicrobial potential of silver nanowires. Nevertheless, the proposed antimicrobial and wound-healing functions should be supported by complementary biological and microbiological evaluations [31].

3.2 SEM-EDX images of nanofibrous membranes

The surface of the membrane formed had observable fine threads due to the electrospinning process, as shown in Figure 5. Nevertheless, for the experiment at Reynolds number of 2 × 106, the angle of attack was limited to α = 23°. The morphology and diameter distribution of the PVA membrane are shown in Figure 5(a). The diameter of all SEM-scanned nanofiber samples was manually measured using ImageJ software, with 50 measurements each. From these measurements, the average diameter of each nanofiber sample was determined. Based on the result, ImageJ showed that the PVA fiber has a diameter 259 ± 8 nm, while the results of measurement and processing with the Gaussian curve approach obtained an average size along with the nanofiber errors. Aside from morphology, the figure also shows the distribution graph of the nanofiber diameter of the PVA membrane. The obtained minimum diameter was 144 nm, and maximum was 449 nm, while the morphology and diameter distribution as shown in Figure 5(b) indicated that PVA/S fiber has a diameter of 172 ± 9 nm. From the measurement and processing results using the Gaussian curve approach, the average size and rectification of the PVA/S membrane nanofiber were also obtained. The minimum diameter of the membrane nanofiber was 122 nm, while the maximum was 257 nm.

Meanwhile, the morphology and diameter distribution of the PVA/AgNWs membrane in Figure 5(c) shows that PVA/AgNWs fiber has a diameter 219 ± 10 nm. The minimum diameter of the PVA/S membrane nanofiber was 142 nm and the maximum was 310 nm. The morphology and diameter distribution of the PVA/S/AgNWs membrane are shown in Figure 5(d). From the results of ImageJ measurements, the PVA fiber has a diameter 217 ± 11 nm, while the measurement and processing with the Gaussian curve approach, obtained the average size along with the nanofiber errors.

The SEM-EDX results of the PVA nanofiber as shown in Figure 5(e) show that the elements contained in the PVA nanofiber are 55.37% carbon (C), 44.41% oxygen (O), and 0.52% sodium (Na). The elemental content of the PVA/S nanofiber shows that bitter leaf has a high silica (Si) content as shown in Figure 5(f). The silica content of PVA/S nanofiber reaches 42.09% with other elements derived from PVA such as C = 9.82%, O = 47.42% and Na = 0.67%. The element content using EDX of the PVA/AgNWs Nanofiber in Figure 5(g) shows that there are several elements such as Ag = 52.45%, O = 14.35%, C = 18.55%, aluminum (Al) = 3.33 %, copper (Cu) = 0.97%, cadmium (Cd) = 7.62%, and argon (Ar) 2.73%. Finally, the elemental content of the PVA/S/AgNWs nanofiber as shown in Figure 5(h) consists of C = 8.89%, O = 49.77%, Na = 0.99%, Si = 38.89% and Ag = 1.86%. From the EDX results, it can be confirmed that Ag, PVA and sambiloto leaf have antibacterial properties which can kill and inactivate bacteria found in incision wounds.

The Ag percentages obtained from EDX represent the elemental composition within the specific region analyzed and should not necessarily be interpreted as the total bulk concentration of Ag throughout the membrane. Differences in sampling location, surface morphology, nanowire distribution, and local composition can significantly affect EDX measurements. Furthermore, wound healing performance is not determined solely by the amount of silver. The PVA/S/AgNWs membrane contains sambiloto extract, which may contribute bioactive phytochemicals associated with antioxidant, anti-inflammatory, and tissue repair processes. Therefore, the superior wound healing response observed for PVA/S/AgNWs may arise from the combined contributions of the nanofibrous PVA structure, AgNWs, and sambiloto-derived bioactive compounds rather than from silver content alone.

Sambiloto leaves potentially contain silicon (Si), which can be one of the constituent mineral components. Based on X-ray fluorescence (XRF) analysis, The presence of Si in A. paniculata leaves at a concentration of approximately 2.7 mg·kg^{-1}. This value places silicon as one of the elements with a relatively high concentration after calcium (64 mg·kg^{-1}) in the analyzed sample. This finding indicates that sambiloto leaves contain Si, although the concentration is relatively low and can not yet be directly interpreted as silica (SiO_2) content. Another study on A. paniculata showed that this plant is able to accumulate silicon after silicate compound treatment, indicating the plant's ability to absorb and distribute Si to plant tissues. Therefore, further characterization is needed to determine the chemical form and phase of silicon naturally present in sambiloto leaves, especially when directed as a precursor in the synthesis of silica or nanosilica [32,33].

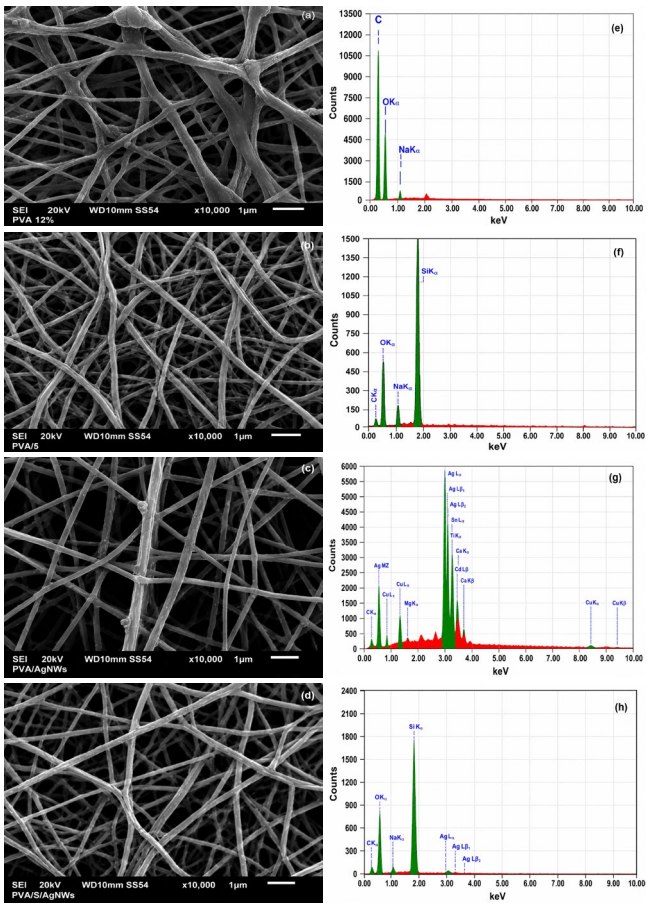


Figure 5. SEM images of nanofiber: (a) PVA, (b) PVA/S, (c) PVA/AgNWs, (d) PVA/S/AgNWs, EDX result of nanofiber:, (e) PVA, (f) PVA/S, (g) PVA/AgNWs, and (h) PVA/S/AgNWs.

The EDX spectrum was predominantly characterized by Ag peaks, confirming the presence of silver in the synthesized nanowires. The detected C and O signals may originate from the PVP capping agent, carbon-containing mounting materials, or the substrate. The apparent Cd and Ar signals observed near the ~3 keV region should be interpreted with caution due to the possibility of overlapping characteristic X-ray emission lines and limitations in automated peak deconvolution. Since Cd and Ar were not used as precursors in the polyol synthesis, these signals cannot be conclusively attributed to the intrinsic composition of the AgNWs without further verification. Therefore, the apparent Cd and Ar peaks may arise from spectral overlap, peak-fitting artifacts, instrumental contributions, or possible contamination. Further confirmation using raw EDX spectra, elemental mapping, and quantitative analysis is recommended [34].

3.3 Nanofibrous membranes

The PVA/S/AgNWs nanofiber produced had a diameter ranging from 146 nm to 337 nm. For preclinical testing, the wound cover demonstrated in Figure 6 shows that the electrospun nanofibrous membrane is attached to the center of the plaster.

Figure 6 represents the membranes of PVA, PVA/S, PVA/AgNWs, and PVA/S/AgNWs, respectively. Each membrane measures 1.25 cm^2 and is attached to the plaster as a wound covering. The antimicrobial activity of AgNWs nanofibers is closely related to the release of Ag^+ ions from the metallic Ag surface. In aqueous environments, surface oxidation of Ag^0 can generate Ag^+ ions, which subsequently interact with bacterial cell membranes and intracellular biomolecules, leading to membrane disruption, oxidative stress, and inhibition of cellular metabolism. Therefore, the Ag^+ release profile can provide important insights into the antimicrobial mechanism of AgNW nanofibers. The release rate is influenced by the accessible surface area of the nanowires, nanowire diameter, degree of aggregation, surface oxidation, and environmental conditions such as pH and ionic strength. A positive correlation between cumulative Ag^+ release and bacterial inhibition would indicate that Ag^+ ions play an important role in the antimicrobial activity. Nevertheless, the antimicrobial effect may also involve direct contact between AgNWs and bacterial cells and the generation of reactive oxygen species. Accordingly, Ag^+ release studies should be combined with antimicrobial assays to establish a comprehensive relationship between silver ion availability and antibacterial performance [35].

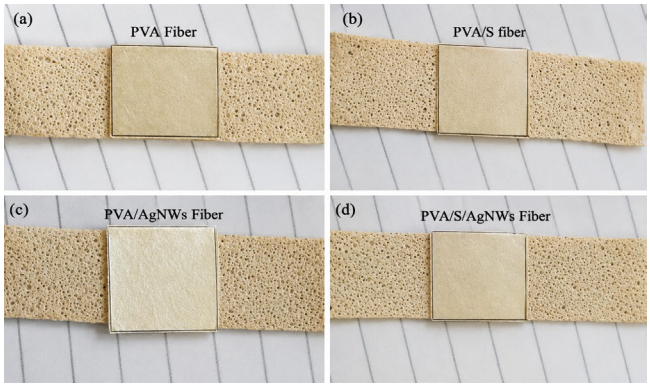


Figure 6. Cover the wound from of (a) PVA, (b) PVA/S, (c) PVA/AgNWs, and (d) PVA/S/AgNWs



Figure 7. The process of shaving the mice's hair (a) veet products, (b) the process of giving veets and (c) the mice that have been shaved.

3.4 Preclinical test

The preparation stages for testing the nanofiber membrane before use in pre-clinical trials are shown in Figure 7. These stages include preparing the tools and materials, removing hair from the skin area to be injured, and making incisions in the test animals with a length ranging from 10 mm to 12 mm. Next, the membrane is applied to the wound area of the test animals as a wound dressing system during the observation period.

Figure 7(a–c) illustrates the preparation, installation, and fixation process of the nanofiber membrane on the wound area as part of the pre-clinical testing procedure. This stage ensures that the membrane can be applied consistently to the wound area so that the effectiveness of each formulation can be compared more objectively. The PVA/S/AgNWs membrane is specifically expected to provide more comprehensive functions because it combines the matrix-forming properties of PVA, the potential biological activity of sambiloto bioactive compounds, and the potential antimicrobial activity of AgNWs. In this stage, the preparation stage is an important part before pre-clinical observations of the wound healing process are carried out. The installed membrane is then observed at certain time intervals to evaluate changes in wound conditions, such as wound size or length, erythema (redness), edema (swelling), and changes in wound surface morphology. The effectiveness of wound healing in mice as shown in Figure 8.

After the fine hairs on the back of the mice were shaved, an incision was made on the back, followed by observation, which was carried out on membrane preparations with four kinds of material variations and one sample without membrane, namely PVA, PVA/S, PVA/AgNWs, PVA/S/AgNWs, as well as the control. Parameters in preclinical testing include the presence of erythema, oedema, and wound length as shown in Figure 8(a) shows the process of wound healing in white rats without being given PVA membrane, AgNWs or Sambiloto (only covered with a plaster). The process of wound healing does occur but requires quite a long time. Figure 8(b) shows the observation of the incision before and after being given the wound covering drug from the PVA nanofiber.

Figure 8(b) shows that the incision experienced wound healing, marked by a reddish color (erythema) that is disappearing and the reduced length. As shown in Figure 8(c), the PVA/S nanofiber experienced accelerated and complete wound closure at 72 h. After 24 h, oedema began to appear, showing cells from the blood circulation to the interstitial tissue with marked scar tissue formation or fibrosis. This scar tissue is a substitute for the skin that has an incision, and the observation for the PVA/AgNWs group is presented in Figure 8(d).

The incision experienced wound healing, marked by disappearing redness (erythema), while oedema in the area around the wound indicated that scar tissue has formed to replace the skin that was injured, as shown in Figure 8(d). The preclinical test observation results of the control group are presented in Figure 8(e). Its shows that the PVA/S/

AgNWs group experienced accelerated wound closure as shown in the decreased wound length. Wound closure occurred because cells from circulating blood to the interstitial tissue were marked by the scar tissue formation or fibrosis. The picture shows that the erythema at 72 h observation was still very clear, while the oedema in the area around the cut was also enlarged. Furthermore, observation at 72 h showed that the cut on the back of the mice did not show the occurrence of wound closure. In this study, we tried to test various samples of wound dressings that we made. From the test results it is shown that the PVA/S/AgNWs sample is almost the same as the PVA/AgNWs or PVA/S sample. This is because the antibacterial properties of the three materials we use (PVA, S and Ag) have worked optimally for the wound healing process. The mean comparison of the erythema and oedema scores is shown graphically in Figure 9.

The preclinical test results of the control group, as presented in Figure 9, show that the erythema at the 72 h was still very clear, while the oedema in the area around the cut was also enlarged. After 72 h the cut on the back of the mice did not show the occurrence of wound closure. The preclinical test results with the given while the erythema and oedema scores in the table were performed using the scale in Table 2.

The wound healing was observed from erythema, oedema, and closure, while Table 2 shows the observation results obtained from 25 mice. The administration of wound closure drug using PVA membranes showed mild erythema at 72 h, while PVA/S and PVA/AgNWs indicated mild erythema at the 48 h. At the beginning of treatment, the average value of the erythema score was 2.6, while PVA/S/AgNWs showed very mild erythema at 48 h with an average score of 3. At 72 h, the erythema control group showed moderate to severe value. This indicates that the PVA/S/AgNWs membrane is better compared to the other wound-covering drugs while the erythema and oedema scores in the table were performed using the scale in Table 3.

Figure 9(a) shows that oedema occurred at 24 h, when the incision still has erythema. Oedema is caused by hyperemia and mostly due to the delivery of fluids as well as cells from the bloodstream to the interstitial tissues. The longer the observation time in the control group, the more visible the oedema around the wound. This was due to the absence of tannin compounds that inhibit mucosal fluid hypersecretion and neutralize inflammatory proteins. Furthermore, tannin has an affinity for protein, hence, it is more concentrated in the wound area. Table 2 shows the mean scores of erythema and oedema that occurred in the mice injured at 0 h, 24 h, 48 h, and 72 h of observation, while the mean length values of each treatment group are shown in Table 4. A comparison of the lengths of wounds of each treatment group is presented graphically in Figure 10.

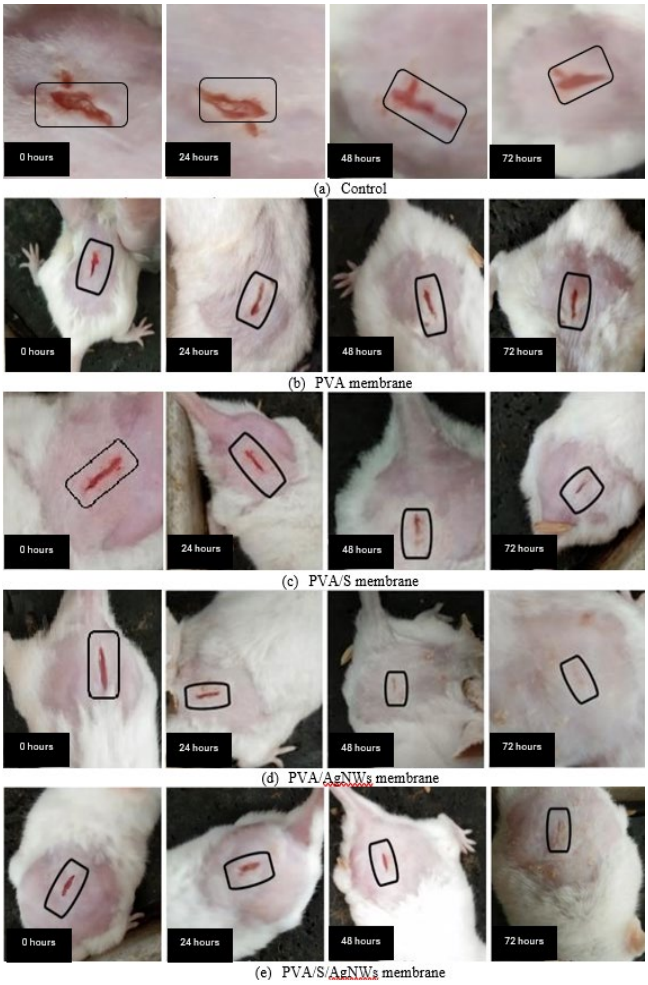


Figure 8. The effectiveness of wound healing in mice.

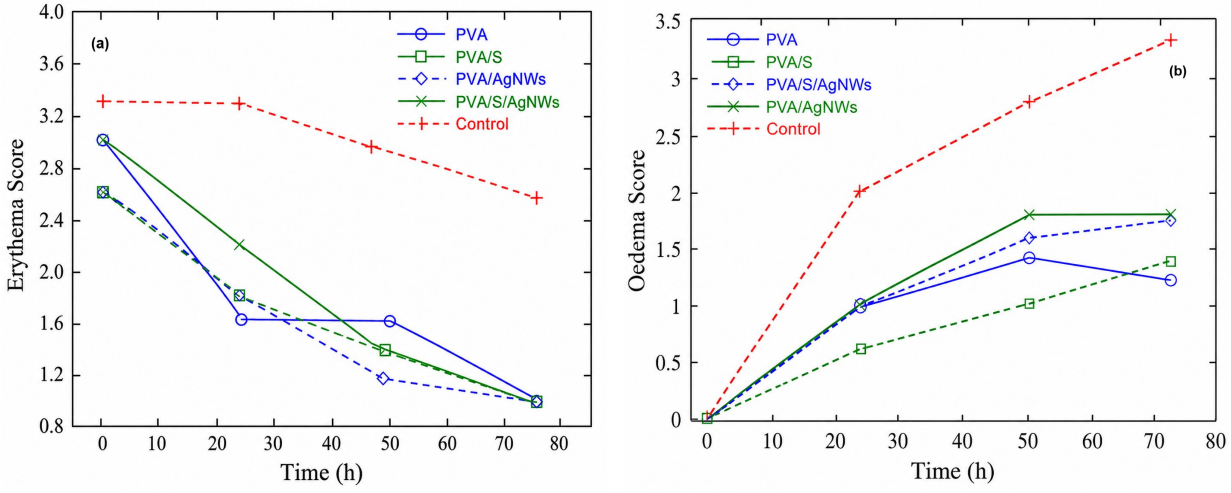


Figure 9. The comparison graph of the mean score of (a) erythema, and (b) Oedema for each treatment.

Table 2. Mean erythema and oedema scores.

Membrane	Observation time [h]							
	0		24		48		72	
	Eri	Ede	Eri	Ede	Eri	Ede	Eri	Ede
PVA	3.0	0.0	1.6	1.0	1.6	1.4	1.0	1.2
PVA/S	2.6	0.0	1.8	0.6	1.4	1.0	1.0	1.4
PVA/AgNWs	2.6	0.0	1.8	1.0	1.2	1.8	1.0	1.8
PVA/S/AgNWs	3.0	0.0	2.2	0.8	1.4	1.6	1.0	1.8
Control (no membrane)	3.4	0.0	3.4	2.0	3.0	2.8	2.6	3.4

Table 3. Draize-FHSA scoring system.

Scoring	Skin reactions	
	Formation of erythema and deep sores	Oedema formation
0	No erythema was formed	Oedema was not observed
1	Very mild erythema	Very mild oedema
2	Erythema was obvious	Edema is mild (the edge of the oedema area was clearly raised)
3	Moderate to severe erythema	Moderate oedema (height of the edge in the edema area was >1 mm)
4	Severe erythema (purplish red color) to mild eschar formation (deep wound)	Severe edema (the height of the edge in the oedema area was >1 mm and extends to the outer area of the exposure)

Table 4. Average wound lengths for each treatment.

Membrane	The length of the incision [mm] for observation time [h]			
	0	24	48	72
PVA	9.0	7.2	5.0	4.6
PVA/S	8.8	7.2	5.4	4.0
PVA/AgNWs	8.8	8.2	6.0	4.8
PVA/S/AgNWs	9.8	7.4	6.6	4.4
Control (no membrane)	9.4	7.8	6.6	6.2

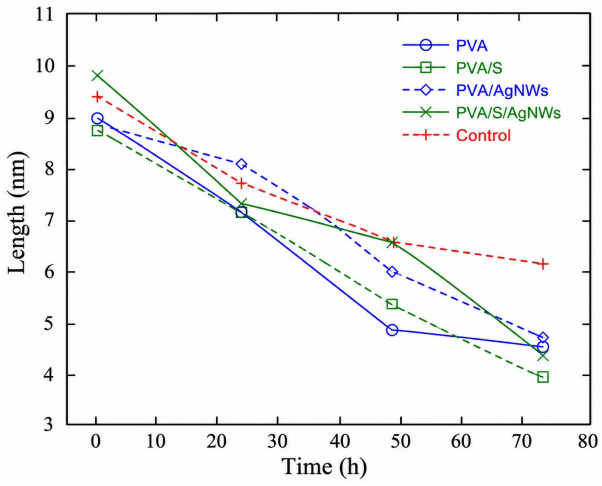


Figure 10. The comparison graph of the mean length of each wound for treatment.

Figure 10 shows that the incisions treated with the wound covering drug with the PVA/S/AgNWs membrane closed quicker than others treated with PVA, PVA/S, and PVA/AgNWs as well as the control. One of the properties of PVA is that it has good oxygen permeability [36,37]. This property is needed by wound covering drug to increase the oxygen pressure outside the wound surface. Sambiloto is an andrographolide compound used to fight disease due to its antibacterial power as well as the potential to activate lymphocytes and produce antibodies. The anti-inflammatory properties inhibit edema through a mechanism that involves the adrenal glands, while the pharmacological effects caused by the active ingredients stimulate the phagocytosis of white blood cells, which play a role in the wound healing process [38–40].

Silver has been used extensively in clinical equipment as an antimicrobial commonly used to treat infections in open wounds and chronic ulcers. It is effective against a variety of aerobic, anaerobic, gram-negative, and gram-positive bacteria, as well as fungi and viruses. Apart from being antimicrobial, silver also has anti-inflammatory properties, as demonstrated by the loss of erythema in chronic wounds treated with colloidal silver. Furthermore, silver in the membrane promotes healing, minimizes pain, prevents infection, produces less scarring, is cheap and easy to use [41–44]. Antibacterial activity test through absorption and turbidity methods against *S. aureus* and *E. coli* showed that the PVA/AgNWs nanofiber had excellent antimicrobial activity [45]. This activity is due to the synergistic effect of PVA and AgNWs, therefore, when used as a primary wound cover, the product acts as a barrier that protects the wound from bacteria [46–48].

The parameters examined in this study include the presence of erythema, oedema, and wound closure. Based on observations with 25 mice and 5 treatments, it was concluded that PVA/S/AgNWs was more effective for wound covering medicine than the other membranes. This was indicated by a very light erythema score starting at 48 h and faster wound closure compared to the incision wounds treated with PVA, PVA/S, and PVA/AgNWs membranes as well as the control. This occurred because the PVA/S/AgNWs membrane contains the content found in PVA, sambiloto leaves, and silver [49–52]. In the controls, the mice had the greatest erythema and oedema scores, as well as the longest wound closure time. This is because they were not given

any treatment to facilitate the wound healing process. Nevertheless, the process in the controls was still ongoing, as demonstrated by the appearance of clinical symptoms from an inflammatory reaction that reduced the size of the cut, indicating that the healthy body had the natural ability to heal itself [53,54].

The electrospinning process produced a membrane with four variations, namely PVA, PVA/S, PVA/AgNWs, and PVA/S/AgNWs, which can be used for wound covering drugs. The morphological analysis results using a binocular microscope showed that the membrane was formed from fine threads due to electrospinning. Preclinical testing for the back cuts of the treated mice began to close at 72 h. Based on the results, the PVA/S/AgNWs membrane was more effective for wound closure than PVA, PVA/S, and PVA/AgNWs membranes. The potential of sambiloto as an ingredient in a wound covering drug is relatively large, as shown in the closure speed when treated with variations of sambiloto, namely PVA/S and PVA/S/AgNWs in the observation of wound length. When the processed product is used as a medical textile, aside from increasing its added value, it is expected to substitute imported products. Furthermore, longer-term observations are necessary to comprehensively evaluate the wound healing process, including re-epithelialization, collagen deposition, tissue remodeling, and subsequent tissue regeneration.

When compared with previously reported electrospun wound dressing systems, the developed AgNW–based membrane demonstrates promising potential for wound healing applications. For instance, a Panax notoginseng@Ag core–shell electrospun nanofiber membrane exhibited a wound residual area of only 1.52% on day 9 and achieved nearly complete wound closure by day 12 in a murine wound model. Similarly, a silver nanoparticle-containing polyurethane electrospun membrane with collagen modification showed approximately 100% inhibition of bacterial growth and enhanced wound healing compared with conventional gauze and commercial collagen sponge dressings. These findings indicate that the incorporation of silver-based nanomaterials into electrospun fibrous matrices can provide multifunctional characteristics relevant to wound management. Nevertheless, quantitative comparison between the present AgNW–based membrane and previously reported electrospun wound dressings should be interpreted cautiously because differences in material composition, nanofiber diameter, silver content, fabrication parameters, wound model, animal species, observation period, and evaluation methods can substantially influence the reported outcomes. Thus, the present comparison serves primarily to contextualize the performance of the developed membrane rather than to establish direct superiority over previously reported systems [55,56].

The wound healing performance of the developed membrane may be associated with the complementary biological functions of AgNWs and sambiloto extract. AgNWs have been reported to exhibit antimicrobial activity through mechanisms involving Ag^+ release and interactions between silver species and microbial cells, while the antimicrobial activity of AgNWs may also be influenced by their physicochemical characteristics and surface properties [57,58]. On the other hand, sambiloto contains several bioactive phytochemicals, particularly andrographolide and related diterpenoid lactones, as well as flavonoids and other phenolic compounds, which have been associated with antimicrobial, antioxidant, and anti-inflammatory activities. Andrographolide, in particular, has been reported to possess antioxidant and anti-inflammatory properties that may be relevant to the regulation of oxidative stress and inflammatory responses [59].

The simultaneous incorporation of AgNWs and sambiloto extract into the nanofibrous membrane may therefore provide complementary biological functions that potentially contribute to improved wound healing. AgNWs may help reduce microbial burden through silver-mediated antimicrobial mechanisms, whereas bioactive compounds from sambiloto extract may contribute to antioxidant and anti-inflammatory responses during the wound healing process. These complementary effects could potentially enhance the overall therapeutic performance of the membrane compared with the individual components. However, the present study did not include a dedicated experimental design to quantitatively distinguish a synergistic effect from an additive or independent effect. Therefore, the observed wound healing response should not be interpreted as definitive evidence of synergy. Instead, the present findings suggest a potential synergistic or complementary interaction between AgNWs and sambiloto extract.

To establish true synergism, future studies should directly compare AgNW–only, sambiloto extract-only, and combined AgNW/sambiloto treatments under identical experimental conditions. The evaluation should include direct antibacterial assays, antioxidant activity, Ag^+ release, cytocompatibility, inflammatory markers, collagen deposition, and wound closure. A factorial experimental design could further determine whether a statistically significant interaction exists between the AgNW and sambiloto factors. Such an approach would provide stronger evidence to distinguish synergistic effects from simple additive effects and would clarify the individual contribution of each component to the wound healing performance of the developed membrane [60].

The superior wound healing performance of PVA/S/AgNWs may result from the complementary contribution of the PVA nanofibrous structure, AgNWs, and bioactive compounds from sambiloto extract. The electrospun nanofibrous architecture may provide a favorable structural environment, while sambiloto-derived phytochemicals may support the wound healing process. AgNWs may additionally contribute to the biological functionality of the membrane. Therefore, relatively small differences in basic characterization parameters may still result in differences in biological performance. Although AgNWs have considerable potential for biomedical applications due to their electrical, optical, and antimicrobial properties, their potential cytotoxicity must be carefully considered. The biological effects of silver nanomaterials are generally associated with the release of Ag^+ ions, generation of reactive oxygen species (ROS), oxidative stress, disruption of cellular membranes, mitochondrial dysfunction, and interactions with intracellular proteins and nucleic acids. For AgNWs, the extent of cytotoxicity may be influenced by several factors, including nanowire concentration, diameter and length, surface coating, aggregation, exposure duration, and the rate of Ag^+ release. The presence of surface coatings or capping agents may alter the interaction between AgNWs and cells and consequently affect their biological responses [61].

In the context of wound dressing applications, the antimicrobial properties of AgNWs may be advantageous because they can help reduce microbial colonization and infection at the wound site. However, excessive release of Ag^+ may also adversely affect mammalian cells involved in tissue repair, including fibroblasts and keratinocytes, potentially interfering with cell proliferation, migration, and tissue

regeneration. Therefore, the concentration and release kinetics of Ag^+ should be carefully controlled to achieve an appropriate balance between antimicrobial efficacy and cytocompatibility [62]. The incorporation of AgNWs into a polymeric membrane may provide an opportunity to regulate silver exposure by controlling AgNW loading, surface accessibility, and the characteristics of the polymer matrix.

For the present AgNW–based membrane, the potential cytotoxicity associated with silver nanowires should therefore be considered when interpreting its suitability for biomedical applications. Although the observed wound healing response suggests promising potential, wound healing observations alone are insufficient to establish the biocompatibility or long-term safety of the developed membrane. Since direct cytotoxicity and cell viability assays were not conducted in the present study, the biocompatibility of the membrane cannot be conclusively established. Further studies should therefore evaluate cell viability and proliferation using relevant skin or wound-healing cell models, such as fibroblasts and keratinocytes, using standardized assays such as MTT, CCK–8, or Live/Dead staining. In addition, evaluating Ag^+ release kinetics alongside cytotoxicity would provide important information regarding the relationship between silver ion exposure, antimicrobial efficacy, and cellular response [63]. Such studies are essential to establish an appropriate therapeutic window in which the AgNW-based membrane provides effective antimicrobial protection while maintaining sufficient cytocompatibility for tissue regeneration.

4. Conclusion

Based on the observed reduction in wound length and macroscopic wound healing responses, the wound healing performance of the treatment groups can be comparatively ranked as follows: PVA/S/AgNWs > PVA/AgNWs > PVA/S > PVA. Among the investigated formulations, the PVA/S/AgNWs membrane demonstrated the most promising wound healing response, suggesting that the incorporation of both AgNWs and sambiloto extract may provide complementary biological functions in the wound healing process. The PVA/AgNWs membrane showed the next best performance, followed by PVA/S, whereas the pure PVA membrane exhibited the lowest performance among the treated groups. However, this ranking is based on the observed experimental trends and should not be interpreted as statistically significant without further quantitative statistical validation. Future studies should incorporate standardized digital wound imaging and calculate wound area reduction (%) to provide a more objective and quantitative comparison of wound closure among treatment groups.

Acknowledgements

The authors are grateful to Budi Khoiri Ardiansyah, a student of the Department of Biology, Faculty of Mathematics and Natural Sciences, University of Lampung who helped in the preclinical test process on the mice. This work was supported by a research grant of Fundamental Research, Contract No. 057/E5/PG.02.00.PL/2024 by the Ministry of Research, Technology and Higher Education of the Republic of Indonesia via the Institute for Research and Community Services of Universitas Lampung by contract No. 574/UN26.21/PN/2024.

References

[1] S. Guo, and L. A. DiPietro, "Factors affecting wound healing," *Journal of Dental Research*, vol. 89, no. 3, pp. 219–229, 2010.

[2] S. A. Eming, P. Martin, and M. Tomic-Canic, "Wound repair and regeneration: Mechanisms, signaling, and translation," *Science Translational Medicine*, vol. 6, no. 265, p. 265sr6, 2014.

[3] S. Dhivya, V. V. Padma, and E. Santhini, "Wound dressings—A review," *BioMedicine*, vol. 5, no. 4, pp. 22–29, 2015.

[4] J. S. Boateng, K. H. Matthews, H. N. E. Stevens, and G. M. Eccleston, "Wound healing dressings and drug delivery systems: A review," *Journal of Pharmaceutical Sciences*, vol. 97, no. 8, pp. 2892–2923, 2008.

[5] G. D. Winter, "Formation of the scab and the rate of epithelization of superficial wounds in the skin of the young domestic pig," *Nature*, vol. 193, pp. 293–294, 1962.

[6] S. P. Miguel, D. R. Figueira, D. Simões, M. P. Ribeiro, P. Coutinho, P. Ferreira, and I. J. Correia, "Electrospun polymeric nanofibres as wound dressings: A review," *Colloids and Surfaces B: Biointerfaces*, vol. 169, pp. 60–71, 2018.

[7] S. Barrientos, O. Stojadinovic, M. S. Golinko, H. Brem, and M. Tomic-Canic, "Growth factors and cytokines in wound healing," *Wound Repair and Regeneration*, vol. 16, no. 5, pp. 585–601, 2008.

[8] K. Jarukamjorn, and N. Nemoto, "Pharmacological aspects of *Andrographis paniculata* on health and its major diterpenoid constituent andrographolide," *Journal of Health Science*, vol. 54, no. 4, pp. 370–381, 2008.

[9] P. K. Singha, S. Roy, and S. Dey, "Antimicrobial activity of *Andrographis paniculata*," *Fitoterapia*, vol. 74, no. 7–8, pp. 692–694, 2003.

[10] J. Lee, Y. D. Suh, J. Lee, P. Lee, S. Han, S. Hong, J. Yeo, H. Lee, and S. H. Ko, "Recent progress in silver nanowire based flexible electrodes," *Journal of Materials Chemistry C*, vol. 6, pp. 7445–7461, 2018.

[11] T. Tomiyama, I. Mukai, H. Yamazaki, and Y. Takeda, "Optical properties of silver nanowire/polymer composite films: Absorption, scattering, and color difference," *Optical Materials Express*, vol. 10, no. 12, pp. 3202–3214, 2020.

[12] S. Hou, J. Liu, F. Shi, G.-X. Zhao, J.-W. Tan, and G. Wang, "Recent advances in silver nanowires electrodes for flexible organic/perovskite light-emitting diodes," *Frontiers in Chemistry*, vol. 10, p. 864186, 2022.

[13] S. Chernousova, and M. Epple, "Silver as antibacterial agent: Ion, nanoparticle, and metal," *Angewandte Chemie International Edition*, vol. 52, no. 6, pp. 1636–1653, 2013.

[14] I. Sondi, and B. Salopek-Sondi, "Silver nanoparticles as antimicrobial agent: A case study on *E. coli* as a model for Gram-negative bacteria," *Journal of Colloid and Interface Science*, vol. 275, no. 1, pp. 177–182, 2004.

[15] D. H. Reneker, and I. Chun, "Nanometre diameter fibres of polymer, produced by electrospinning," *Nanotechnology*, vol. 7, no. 3, pp. 216–223, 1996.

[16] S. Ramakrishna, K. Fujihara, W.-E. Teo, T. Yong, Z. Ma, and R. Ramaseshan, "Electrospun nanofibers: Solving global issues," *Materials Today*, vol. 9, no. 3, pp. 40–50, 2006.

[17] Y. Si, X. Tang, J. Yu, and B. Ding, "Electrospun nanofibers: Solving global issues," in *Electrospun Nanofibers for Energy and Environmental Applications*. Berlin, Germany: Springer, pp. 3–38, 2014.

[18] E. A. Kamoun, S. A. Loutfy, Y. Hussein, and E.-R. Kenawy, "Recent advances in PVA-polysaccharide based hydrogels and electrospun nanofibers in biomedical applications: A review," *International Journal of Biological Macromolecules*, vol. 187, pp. 755–768, 2021.

[19] Y. Yang, Z. Zhang, M. Wan, Z. Wang, X. Zou, Y. Zhao, and L. Sun, "A facile method for the fabrication of silver nanoparticles surface decorated polyvinyl alcohol electrospun nanofibers and controllable antibacterial activities," *Polymers*, vol. 12, p. 2486, 2020.

[20] K. T. Cao, K. K. Tran, and H. T. Do, "Polyol method and surface functionalization of silver nanowires using bovine serum albumin for surface-enhanced Raman scattering application," *Journal of Metals, Materials and Minerals*, vol. 33, no. 3, p. 1727, 2023.

[21] J. Junaidi, K. Triyana, E. Suharyadi, H. Harsojo, and L. Y. L. Wu, "The roles of polyvinyl alcohol (PVA) as the capping agent on the polyol method for synthesizing silver nanowires," *Journal of Nano Research*, vol. 49, pp. 174–180, 2017.

[22] J. Junaidi, M. W. Saputra, R. Marjunus, S. Sembiring, and S. Hadi, "The quenching and sonication effect on the mechanical strength of silver nanowires synthesized using the polyol method," *Molecules*, vol. 26, p. 2167, 2021.

[23] J. Junaidi, D. A. Malik, M. Rizki, I. Pratiwi, I. Karo-Karo, R. Marjunus, D. Asmi, and S. Hadi, "Synthesis of silver nitrate by evaporation chemical reduction process as potential materials for silver nanowires application," *Science and Technology Indonesia*, vol. 9, no. 3, pp. 642–650, 2024.

[24] C.-W. Li, R. Fu, C. Yu, Z.-H. Li, H. Guan, D.-Q. Hu, D.-H. Zhao, and L.-C. Lu, "Silver nanoparticle/chitosan oligosaccharide/poly(vinyl alcohol) nanofibers as wound dressings: A preclinical study," *International Journal of Nanomedicine*, vol. 8, pp. 4131–4145, 2013.

[25] E. Rahmani, M. Pourmadadi, N. Zandi, A. Rahdar, and F. Baino, "pH-responsive PVA-based nanofibers containing GO modified with Ag nanoparticles: Physico-chemical characterization, wound dressing, and drug delivery," *Micromachines*, vol. 13, no. 11, p. 1847, 2022.

[26] S. Hossain, Z. Urbi, H. Karuniawati, R. B. Mohiuddin, A. M. Qrimida, A. M. M. Allzrag, L. C. Ming, E. Pagano, and R. Capasso, "*Andrographis paniculata* (Burm. f.) Wall. ex Nees: An updated review of phytochemistry, antimicrobial pharmacology, and clinical safety and efficacy," *Life*, vol. 11, no. 4, p. 348, 2021.

[27] D. P. Gonde, B. K. Bhole, and K. S. Kakad, "Andrographolide, diterpenoid constituent of *Andrographis paniculata*: Review on botany, phytochemistry, molecular docking analysis, and pharmacology," *Phytochemistry*, vol. 217, p. 113903, 2024.

[28] E. S. Chauhan, K. Sharma, and R. Bist, "Andrographis paniculata: A review of its phytochemistry and pharmacological activities," *Research Journal of Pharmacy and Technology*, vol. 12, no. 2, pp. 891–900, 2019.

[29] A. May, Z. Kopecki, B. Carney, and A. Cowin, "Antimicrobial silver dressings: A review of emerging issues for modern wound care," *ANZ Journal of Surgery*, vol. 92, no. 3, pp. 379–384, 2022.

[30] U. J. M. Ikezu, and S. N. Ugariogu, "Identification, quantification of phytochemicals and elemental analysis from ethanolic leaf extract of *Andrographis paniculata*," *South Asian Research Journal of Natural Products*, vol. 6, no. 3, pp. 144–156, 2023.

[31] S. R. Kumar, A. C. Jnanesha, S. Bharathkumar, K. Sravya, S. Venugopal, and R. K. Lal, "Unveiling the effect of foliar applied siliceous compounds on reducing seed shattering for the conservation of endangered kalmegh (*Andrographis paniculata* (Burm. f.) Wall. ex Nees.)," *Biocatalysis and Agricultural Biotechnology*, vol. 68, p. 103700, 2025.

[32] T. T. Hoang, and T. Q. Tran, "Investigating the effect of capping agent PVP on the synthesis of silver nanowires by polyol method and its application as flexible transparent conducting electrode," *VNUHCM Journal of Science and Technology Development*, vol. 16, no. 4, pp. 52–60, 2013.

[33] J. Daphne, A. Francis, R. Mohanty, N. Ojha, and N. Das, "Green synthesis of antibacterial silver nanoparticles using yeast isolates and its characterization," *Research Journal of Pharmacy and Technology*, vol. 11, no. 1, pp. 83–92, 2018.

[34] Z. Zhang, Y. Wu, Z. Wang, X. Zou, Y. Zhao, and L. Sun, "Fabrication of silver nanoparticles embedded into polyvinyl alcohol (Ag/PVA) composite nanofibrous films through electro-spinning for antibacterial and surface-enhanced Raman scattering (SERS) activities," *Materials Science and Engineering: C*, vol. 69, pp. 462–469, 2016.

[35] Z. W. Abdullah, Y. Dong, N. Han, and S. Liu, "Water and gas barrier properties of polyvinyl alcohol (PVA)/starch (ST)/glycerol (GL)/halloysite nanotube (HNT) bionanocomposite films: Experimental characterisation and modelling approach," *Composites Part B: Engineering*, vol. 74, p. 107033, 2019.

[36] L. V. Hai, L. Zhai, H. C. Kim, J. W. Kim, and J. Kim, "Green nanocomposites made with polyvinyl alcohol and cellulose nanofibers isolated from recycled paper," *Journal of Renewable Materials*, vol. 7, no. 7, pp. 621–629, 2019.

[37] C. J. Tan, and Y. W. Tong, "The effect of protein structural conformation on nanoparticle molecular imprinting of ribonuclease A using miniemulsion polymerization," *Langmuir*, vol. 23, pp. 2722–2730, 2007.

[38] J. M. Yang, W. Y. Su, T. L. Leu, and M. C. Yang, "Evaluation of chitosan/PVA blended hydrogel membranes," *Journal of Membrane Science*, vol. 236, pp. 39–51, 2004.

[39] K. Qiu, and A. N. Netravali, "Halloysite nanotube reinforced biodegradable nanocomposites using noncrosslinked and malonic acid crosslinked polyvinyl alcohol," *Polymer Composites*, vol. 34, pp. 799–809, 2013.

[40] K. Song, Y. Zhang, J. Meng, E. C. Green, N. Tajaddod, H. Li, and M. L. Minus, "Structural polymer-based carbon nanotube composite fibers: Understanding the processing–structure–performance relationship," *Materials*, vol. 6, pp. 2543–2577, 2013.

[41] T. S. Gaaz, A. B. Sulong, M. N. Akhtar, A. A. H. Kadhum, A. B.

Mohamad, and A. A. Al-Amiery, "Properties and applications of polyvinyl alcohol, halloysite nanotubes and their nanocomposites," *Molecules*, vol. 20, no. 12, pp. 22833–22847, 2015.

[42] P. Wang, S. Jiang, Y. Li, Q. Luo, J. Lin, L. Hu, L. Liu, and F. Xue, "Virus-like mesoporous silica-coated plasmonic Ag nanocube with strong bacteria adhesion for diabetic wound ulcer healing," *Nanomedicine: Nanotechnology, Biology and Medicine*, vol. 24, p. 102381, 2021.

[43] T. Jayakumar, C. Y. Hsieh, J. J. Lee, and J. R. Sheu, "Experimental and clinical pharmacology of *Andrographis paniculata* and its major bioactive phytoconstituent andrographolide," *Evidence-Based Complementary and Alternative Medicine*, p. 84670, 2013.

[44] H. Suryanto, M. Muhajir, B. D. Susilo, Y. R. J. Pradana, H. W. Wijaya, A. S. Ansari, and U. Yanuhar, "Nanofibrillation of bacterial cellulose using high-pressure homogenization and its films characteristics," *Journal of Renewable Materials*, vol. 9, no. 10, pp. 1717–1728, 2021.

[45] I. K. Dewi, T. Lestari, and S. N. Rofi'ah, "Formulation and physical test of ethanolic extract sambiloto leaves (*Andrographis paniculata*) ointment," *Sains Medika*, vol. 6, no. 2, pp. 56–60, 2015.

[46] M. Mishra, H. Kumar, and K. Tripathi, "Diabetic delayed wound healing and the role of silver nanoparticles," *Digest Journal of Nanomaterials and Biostructures*, vol. 3, no. 2, pp. 49–54, 2008.

[47] G. K. Devi, P. Suruthi, R. Veerakumar, S. Vinoth, R. Subbaiya, and S. Chozhavendhan, "A review on metallic gold and silver nanoparticles," *Research Journal of Pharmacy and Technology*, vol. 12, no. 2, pp. 935–943, 2019.

[48] J. Jain, S. Arora, J. M. Rajwade, P. Omray, S. Khandelwal, and K. M. Paknikar, "Silver nanoparticles in therapeutics: Development of an antimicrobial gel formulation for topical use," *Molecular Pharmaceutics*, vol. 6, no. 5, pp. 1388–1401, 2009.

[49] B. K. Priyanka, R. P. Ritesh, V. B. Pramod, P. C. Pavan, and N. S. Vinayak, "Silver nanoparticles—A review," *Research Journal of Pharmacy and Technology*, vol. 10, no. 6, pp. 1820–1833, 2017.

[50] F. Paladini, and M. Pollini, "Antimicrobial silver nanoparticles for wound healing application: Progress and future trends," *Materials*, vol. 12, no. 16, p. 2543, 2019.

[51] S. Maheshwari, R. K. Tiwari, and L. Singh, "Green expertise: Synthesis of silver nanoparticles for wound healing application—An overview," *Research Journal of Pharmacy and Technology*, vol. 14, no. 2, pp. 1149–1154, 2021.

[52] N. H. Hoang, V. N. Nguyen, T. T. Nguyen, and T. M. D. Nguyen, "Impact of microwave synthesis time on the shape of silver nanostructures and their antibacterial activity," *Journal of Metals, Materials and Minerals*, vol. 33, no. 1, pp. 101–106, 2023.

[53] Z. Gao, S. Liu, S. Li, X. Shao, P. Zhang, and Q. Yao, "Fabrication and properties of the multifunctional rapid wound healing *Panax notoginseng*@Ag electrospun fiber membrane," *Molecules*, vol. 28, no. 7, Art. no. 2972, 2023.

[54] J.-P. Chen, and Y. Chiang, "Bioactive electrospun silver nanoparticles-containing polyurethane nanofibers as wound dressings," *Journal of Nanoscience and Nanotechnology*, vol. 10, no. 11, pp. 7560–7564, 2010.

[55] T. Toporcer, T. Grendel, B. Vidinskỳ, P. Gál, J. Sabo, and R. Hudák, "Mechanical properties of skin wounds after *Atropa belladonna* application in rats," *Journal of Metals, Materials and Minerals*, vol. 16, no. 1, pp.25–29, 2017.

[56] Y. Wang, G. Yue, H. Lu, Z. Liu, N. Wang, F. Liu, H. Yin, and Y. Zhao, "Wound dressing applications of electrospun nanofibers: mechanism, construction and recent progress," *Nanoscale,* vol. 18, no. 12, pp. 6203–6220, 2026.

[57] R. S. Jones, R. R. Draheim, and M. Roldo, "Silver nanowires: Synthesis, antibacterial activity and biomedical applications," *Applied Sciences*, vol. 8, no. 5, p. 673, 2018.

[58] T. M. S. Vidhya and Geetha, "In vitro evaluation of anti-inflammatory activity of *Andrographis paniculata*," *Research Journal of Pharmacy and Technology*, vol. 11, no. 3, pp. 957–958, 2018.

[59] L. L. Aver'ianova, "Effect of antibiotics on the resistance of white mice to infection caused by antibiotic-resistant *Staphylococcus* strains," *Antibiotiki*, vol. 21, no. 8, pp. 735–742, 1976.

[60] B. Reidy, A. Haase, A. Luch, K. A. Dawson, and I. Lynch, "Mechanisms of silver nanoparticle release, transformation and toxicity: A critical review of current knowledge and recommendations for future studies and applications," *Materials*, vol. 6, no. 6, pp. 2295–2350, 2013.

[61] R. N. Mardiana, and Handayani, "Antibacterial activity of the sambiloto leaf extracts (*Andrographis paniculata*) to *Bacillus cereus* and *Pseudomonas aeruginosa*," *Biofarmasi*, vol. 14, no. 1, pp. 19–24, 2016.

[62] J. Pusmarani, C. Dewi, J. P. Risky, H. A. H. Nur, I. F. Sasri, H. Febrianti, P. Setyo, and I. Zullies, "In vitro and in vivo study of gastroprotective effect of purified extract Andrographis paniculata," *Research Journal of Pharmacy and Technology*, vol. 16, no. 8, pp. 3615–3621, 2023.

[63] N. W. S. D. Arini, B. K. Satriyasa, I. M. Jawi, and A. W. Indrayani, "Comparison of antibacterial activity of sambiloto (Andrographis paniculata) ethanol and water stem extract against methicillin-resistant Staphylococcus aureus (MRSA) ATCC3351 in vitro," *Jurnal Epidemiologi Kesehatan Komunitas*, vol. 5, no. 2, pp. 69–76, 2020.